Contribution to the improvement of thermal comfort in a bioclimatic building by integration of a phase change material.

Yacouba Camara, Xavier Chesneau, Cellou Kante

Contribution to the improvement of thermal comfort in a bioclimatic building by integration of a phase change material

Yacouba Camara[1,2]* , Xavier Chesneau[1], Cellou Kante[2]

The objective of this research is to enable the improvement of energy performance of bioclimatic habitats in tropical hot and humid zones. Numerical modeling of heat transfer phenomena in a stabilized clay brick (BTS) habitat with a transparent tile roofing, a false ceilings containing encapsulated phase change materials and a concrete floor is presented. A study on indoor air temperature distributions was conducted as well as on heat storage in phase change materials and on the storage and restitution efficiencies as a function of thickness. To show the reliability of our research, we validated the chosen model through an experimental study by (Zivkovic and Fujii, 2001). In addition, we did a comparative study between air temperatures for habitats with and without phase change material in the false ceiling to see the existence of thermal comfort in the habitat which is the goal of this study. The values of these air temperatures observed at 16 h in a modern habitat and a conventional habitat are respectively 28,14 °C and 29,02 °C. The values of storage and restitution heat efficiencies in PCM are respectively 25.92% and 19.34% for the first day.

Keywords: Thermal comfort, Heat storage, Bioclimatic habitat

INTRODUCTION

Faced with the rising cost of energy and the negative consequences of greenhouse gas emissions, it has become essential to develop innovative systems that permit to improve energy efficiency, better control of energy demand and a reduction in CO_2 emissions (Bedecarrats, 2010).

The housing sector consumes about 40% of primary energy consumption and contributes up to 33% of greenhouse gas emissions. In addition, almost half of the building's energy consumption is devoted to the air conditioners in developed countries (Ramakrishnan and al., 2017; Pérez-Lombard and al., 2008). Nevertheless, much of

[1] Université de Perpignan Via Domitia, Laboratoire de Mathématiques et Physique, 52 Avenue Paul Alduy 66860, Perpignan, France.
[2] Université Gamal Abdel Nasser, Laboratoire d'Enseignement et de Recherche en Energétique Appliquée, BP 1147, Conakry, Guinée.

the space conditioning energy is ultimately lost through the building envelope due to the lack of thermal inertia in modern buildings. Thus, energy saving and green building design have become an important research area. A common theme among effective building design strategies is the improvement of the thermal mass of the building envelope for storing thermal energy during the day and restitute to the building during the cooler night. This can reduce maximum temperatures and temperature fluctuations inside the habitat (Soares and al., 2013; Baetens and al., 2010).

Bioclimatic architecture, for its part, is a technique whose cost is not too high, which allows to make spectacular savings. A large number of homes built by our ancestors already used this technology: spacious, using quality materials and a good finish. Then the concern for yield and profit has led to the loss of quality, the use of unhealthy and less expensive materials and the reduction of spaces, to obtain what we see today: rabbit cages and villas where it's not good to live (Boukli Hacene, 2013). The application of bioclimatic principles is a factor in reducing energy consumption and CO2 emissions in the construction sector (Tzikopoulos and al., 2005; Manzano-Agugliaro and al., 2015).

Heating, ventilation and air conditioning (HVAC) are the largest energy consumers in the building sector (Hoy-Yen and al., 2010).

The design of buildings is based mainly on energy saving criteria (Berger, 1984); It associates the insulation, solar contributions, inertia with thermal comfort, because it is defined on the one hand as the satisfaction expressed by an individual with respect to the thermal environment of the medium in which it evolves (Boukli Hacene and al., 2011).

The feeling of comfort is a difficult concept to quantify. It depends on a large number of criteria aimed at achieving an adequate thermal equilibrium between the human body and its environment (Brun, 2011).

Thermal comfort is an obvious need and all built structures (habitable sector) or constructed (transport sector) are equipped with systems to heat or cool the indoor climate (Ahmad, 2004; Candas, 2008). Numerous physical or psychophysical studies have shown relationships between the intensity of the sensation and that of the stimulus. The sensation increases according to the intensity of the stimulus, or the gap between the stimulus and a threshold.

In the last twenty years, several forms of bulk encapsulated phase change materials have been marketed for active and passive solar systems, including direct gain. However, the surface of 5

most encapsulated commercial products was insufficient to provide heat to the building after the phase change material was melted by direct sunlight. On the other hand, the walls and ceilings of a building offer large areas of passive heat transfer in each zone of the building (Neeper, 2000).

The integration of phase-change materials in building walls allows a large amount of energy to be stored by latent heat in a small volume of material (Younsi and al., 2009). The special feature for phase change materials is that they can store heat energy by latent heat, as well as by sensible heat (Kuznik and al., 2008). Thermal energy storage is an attractive technology because it is the most appropriate method to correct the gap between energy demand and supply (Oro and al., 2012; Hussein and al., 2014).

Belén Zalba et al. (Zalba and al., 2003) used phase-change materials in free-cooling systems. Free cooling is understood as a means of storing freshness outdoors during the night, to cool the interior of the building during the day. The use of phase change materials is appropriate because of the small difference in temperature between day and night indoors and outdoors.

Mohamed M. Farid et al. (Khudhair and Farid, 2004) have defined that, the latent heat accumulator is one of the most efficient means of storing thermal energy. Unlike the sensible heat storage method, the latent heat storage method provides a much higher storage density, with a lower temperature difference between storage and heat release. Phase change materials can provide a large latent heat storage capacity over the range of temperature typically encountered in buildings, so they can improve the degree of thermal comfort.

Lavinia Socaciu et al. (Socaciu and al., 2014) studied phase change materials in building construction, the study shows that the incorporation of appropriate phase change material into buildings can be an effective solution to reduce energy consumption and cool down the buildings. A small amount of phase change material can lift the thermal inertia substantially without increasing the mass of the structure.

The incorporation of appropriate phase-change materials into walls, ceilings and floors of buildings can directly capture solar energy and store large amounts of thermal energy in the building envelope without the associated large structural mass at sensible heat storage, which helps to reduce the frequency of changes in internal air temperature and keep the temperature close to the desired temperature for a longer period of time (Fang and al., 2008).

Chi-ming Lai et al. studied the thermal performance of a honeycomb aluminum wall panel incorporating microencapsulated phase change material. The honeycomb phase change material module has sufficient heat conduction enhancement. As a result, internal temperatures within the module were similar and did not show latent heat of stratification. This study applied in addition to honeycomb phase change material, has the ability to regulate the temperature of photovoltaic panels, and the results indicated that photovoltaic panels with nest phase change material module of bees have increased the efficiency of the photovoltaic panel generator compared to normal photovoltaic panels attached directly to the exterior wall of a building (Chi-ming and Shuichi, 2014). 6

Y. Zohir et al. (Younsi and al., 2009) have experimentally studied a reduced scale composite-wall containing phase-change materials. In this study, they found that the storage of latent heat thermal energy appears indeed very interesting in comparison with sensible heat storage. The main advantages are the storage of a large amount of heat in a reduced volume of phase change materials and the return to a temperature level close to thermal comfort temperatures.

Alvaro Gracia et al. made a study on phase change materials and thermal energy storage for buildings. In this study, they used the method of integrating phase change materials into the racks of clay bricks to increase energy efficiency in buildings. For this study, they discussed the notions of storage by sensible heat, latent heat and thermochemical reaction. Through this study, they have shown that it is possible to do heating and cooling with thermal energy storage in buildings (Gracia and Cabeza, 2015).

B. Zivkovic et al. made a study on the isothermal phase analysis of phase change materials contained in rectangular and cylindrical containers. The calculation method for the isothermal phase change of encapsulated phase change material in a single container is based on the enthalpy method. The theoretical model was verified with a test problem and an experiment carried out to evaluate the validity of the hypotheses of the mathematical model.

The results obtained with the proposed method show a very satisfactory agreement with the results obtained from other calculation models. In addition, the comparison between the melting time of the phase change materials contained in the rectangular and cylindrical containers was performed and the results show that the rectangular container requires nearly half of the melting time obtained for the cylindrical container with the same volume and the same zone of heat transfer between the coolant and the wall of the container. It is therefore preferable to use rectangular containers to encapsulate the phase change material rather than to the cylindrical containers (Zivkovic and Fujii, 2001).

NUMERICAL METHOD

1. Climatic Data

The data we used for this research are the climatic data of the typical day of March with an overall radiation of 1000 W/m^2 and a maximum and minimum temperature respectively of 35°C and 25°C. These data allow us to find the hourly variations of the ambient temperature and the solar flux by considering a sinusoidal variation (figure 1).

Figure 1 shows the evolution of horizontal global solar flux and ambient air temperature for the typical day in March. Indeed, March is the hottest time of the year for Guinea. We therefore select the climatic data for the typical March day as input to our program as they allow us to analyze the thermal behavior of the habitat for extreme climatic conditions.

Figure 1: Horizontal Global Solar Flux and Ambient Temperature of the Standard Day of March

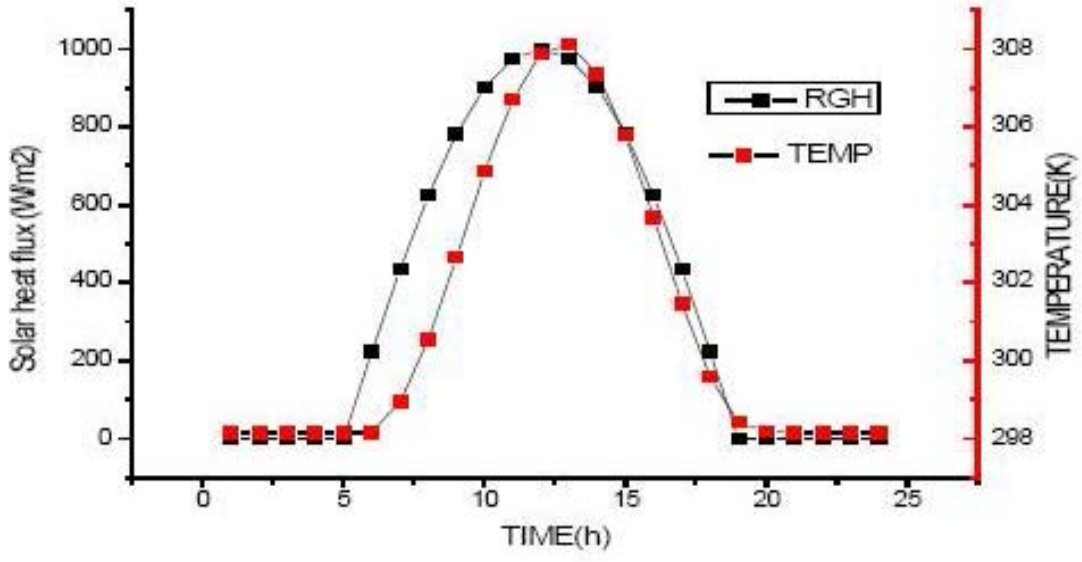

2. Description of the Physical Model of the Bioclimatic Habitat

The bioclimatic roof model we use is a flat solar collector whose roof is made of transparent tiles. Consider, as shown in Figures 2 and 3, a bioclimatic type habitat that can be decomposed into a parallelepiped-shaped enclosure and a roof separated by a rectangular panel containing phase-change materials encapsulated as false ceilings (Figure 4). The roof is likened to a flat wall of rectangular section, inclined at an angle to the horizontal false ceiling, which is extended to a length sufficient to protect the facade of the vertical walls of the parallelepiped enclosure of solar flux.

It is thus composed of an inclined transparent tile plate forming an angle of 30 ° with respect to the horizontal made of a panel of phase-change material and the vertical walls in stabilized earth bricks. Under the roof air circulate in the enclosure by natural convection. The outer face of the roof has transparent tiles. The thermophysical properties of the materials constituting the roof, the false ceiling and the parallelepiped enclosure, assumed to be constant are reported in Table 1.

Figure 2: Diagram of the Roof of the Habitat Model

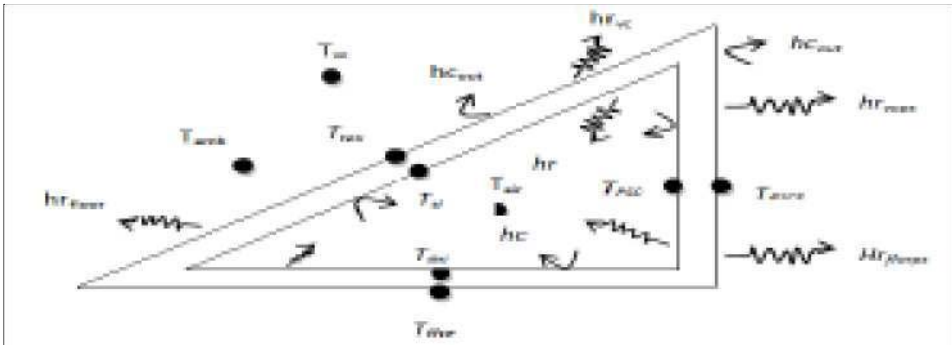

Figure 3: Diagram of the Parallelepiped Enclosure of the Bioclimatic Habitat

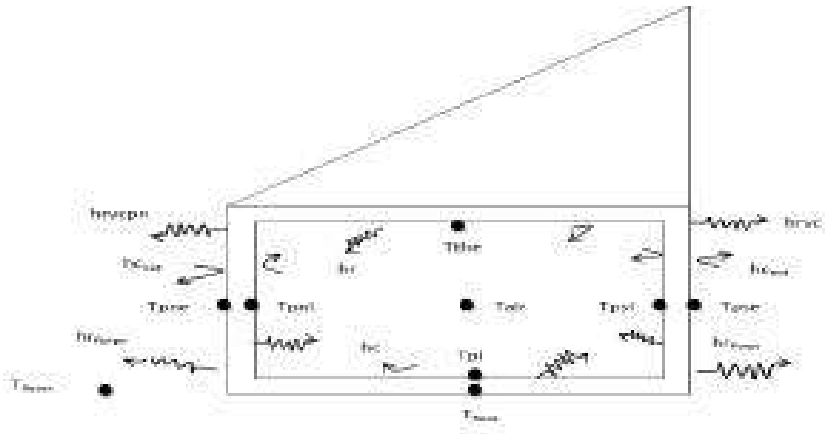

Figure 4: Geometry of the Rectangular Container Containing PCM

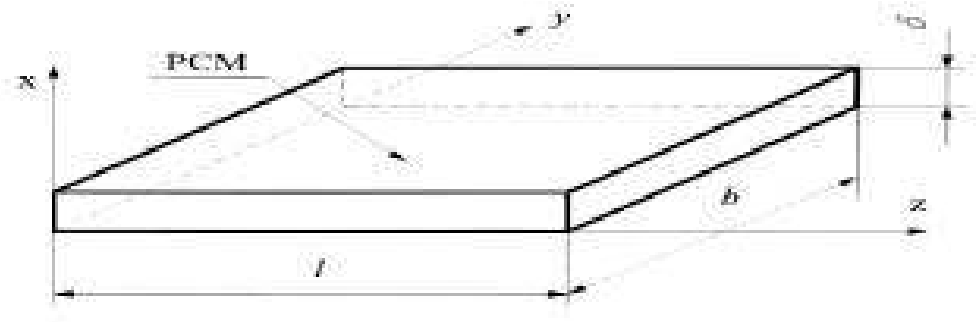

Table 1: Thermophysical Properties of the Materials

Materials	Density 5 (kg/m^3)	Heat Capacity Cp (J/Kg/K)	Thermal Conductivity K (W.m^{-1}.K^{-1})
Transparent tiles	1200	800	0.752
BTS	2000	1500	1.1
Hydrated salt	1710	1400	1.09
Paraffin RT27	870	2400	0.24

Source: Zivkovic and Fujii, 2001; Aadmi and al., 2013; Ouédraogo and al., 2007; Vasilios and Alan, 1993

3. Mathematical Formulation of the Model

3.1 Simplifying Hypotheses

The methodology adopted for describing the thermal behavior of our building model is based on nodal analysis (Kemajou and Mba, 2012).

The detailed study of the heat transfer phenomena involved in the functioning of the building (Figures 2, 3 and 4) leads us to make a number of hypotheses, the main ones being:

1. The heat transfers are unidirectional, perpendicular to the walls
2. The materials are assimilated to gray bodies
3. The thermophysical properties of materials are assumed to be constant
4. The rate of air change is imposed in the enclosure of the building
5. The convective heat transfer between the upper wall of the PCM and the interior air of the roof is neglected
6. The upper wall of the PCM receives a quantity of imposed solar flux
7. The heat transfer mode in the PCM is only conduction

3.2 Basic Equations

The establishment of transfer equations is based on the analogy between thermal and electrical transfers.

In a general way, the instantaneous variation of the energy within a component of the habitat is equal to the algebraic sum of the flux densities exchanged within this component.

It is written:

$$\frac{M_i Cp_i \partial T_i}{s \quad \partial T} = DFSA_i + \sum_{i=1}^{n} \sum_x \varphi_{xij} \qquad ...(1)$$

φ_{xij}: Heat flux density exchanged by the transfer mode x (conduction, convection and radiation) between the media (i) and (j), (W.m^{-2})

S: Wall section (m^2)

$DFSA_i$: Solar flux density absorbed by the material (i) (W.m^{-2})

$$DFSA_i = \alpha_i \varphi_i \qquad ...(2)$$

α_i: Thermal absorption coefficient of the material (i)

φ_i: Solar flux density captured by the surface of the medium (i) (W.m-2).

By introducing an exchange coefficient h_{xij} and by linearizing transfers, we can write:

$$\varphi_{xij} = h_{xij}(T_j - T_i) \qquad ...(3)$$

Thus, the equation 1 is written:

$$\frac{M_i Cp_i \partial T_i}{s \quad \partial T} = DFSA_i + \sum_{i=1}^{n} \sum_x h_{xij}\left(T_j - T_i\right) \qquad ...(4)$$

We will then apply Equation 3 to the various medium of our system.

Exterior wall of building

$$\frac{M_{pex} Cp_{pex}}{s} \frac{\partial T_{pex}}{\partial t} = \alpha_{pex} \varphi_{pex} + \frac{K_{pex}}{Ep_{pex}}\left(T_{pi} - T_{pex}\right)$$

$$+ hc_{ex}\left(T_{amb} - T_{pex}\right) + hr_{vc.pex}(T_{vc} - T_{pex})$$

$$+ hr_{sol,pex} F_{sol}\left(T_{sol} - T_{pex}\right) \qquad ...(5)$$

Building air zone

$$\frac{M_{air} Cp_{air}}{s} \frac{\partial T_{airh}}{\partial t} = \sum_{i=1}^{n} h_{ci,pi}\left(T_{pi} - T_{airh}\right) + \phi_{ra} \qquad ...(6)$$

Internal wall of building

$$\frac{M_{pi} Cp_{pi}}{s} \frac{\partial T_{pi}}{\partial t} = \frac{K_{pi}}{Ep_{pi}}\left(T_{pe} - T_{pi}\right)$$

$$+ hc_i\left(T_{airh} - T_{pi}\right) + \sum_{i=1}^{n} hr_{i \to pi} F_i (T_i - T_{pi}) \qquad ...(7)$$

Air Renewal

Considering a volume of air V exchanged between the outside and the inside of the habitat, this corresponds to a quantity of heat Q in joules. By supposing that volume is exchanged every hour. We will thus have an air exchange flux Φ_{ra} (J.h^{-1}):

$$\phi_{ra} = c\dot{Q}\left(T_{airout} - T_{airins}\right) \qquad ...(8)$$

With:

Q. the volumic flow rate in m^3.h^{-1}

c the heat of the air (c=1225J.m^{-3}.K^{-1}).

T_{airout} ambient air temperature outside the home

T_{airins} air temperature inside the enclosure of the building

3.3 Heat Equation in the Phase Change Material

Continuity of flux at the solid-liquid interface, by posing that the difference between the flux on either side of the interface is equal to the amount of instantaneous heat released or absorbed in the form of phase change heat (Figure 5).

Figure 5: Evolution of the Temperature of the PCM with Phase Change

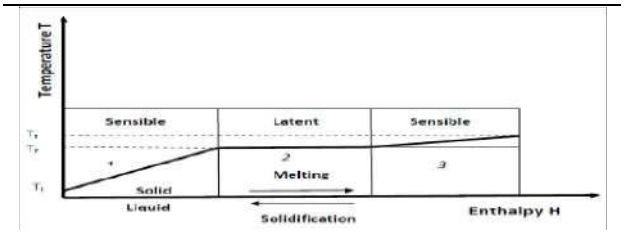

$$\text{If } T \le T_F \quad \frac{\partial T}{\partial t} = \left(\frac{\lambda}{\rho Cp}\right)_s \left(\frac{\partial^2 T}{\partial X^2} + \frac{\partial^2 T}{\partial Y^2}\right) \quad ...(9)$$

$$H_{i,j} = \rho_s Cp_s \left(T_{i,j} - T_{amb}\right) \quad ...(10)$$

Latent Phase

$$\text{If } T \text{ f } T_F \text{ and } H_{i,j} \text{ f } \rho_s Cp_s \left(T_F - T_{amb}\right) \quad ...(11)$$

$$\frac{\partial H}{\partial t} = \lambda_s \left(\frac{\partial^2 T}{\partial X^2} + \frac{\partial^2 T}{\partial Y^2}\right) \quad ...(12)$$

$$H_{i,j}^{t+\Delta t} = \lambda_s \left(\frac{\partial^2 T}{\partial X^2} + \frac{\partial^2 T}{\partial Y^2}\right) \Delta t + H_{i,j}^{t} \quad ...(13)$$

Sensible Phase

$$\text{If } H_{i,j} \text{ f } \rho_s Cp_s \left(T_F - T_{amb}\right) \quad ...(14)$$

$$\frac{\partial T}{\partial t} = \left(\frac{\lambda}{\rho Cp}\right)_s \left(\frac{\partial^2 T}{\partial X^2} + \frac{\partial^2 T}{\partial Y^2}\right) \quad ...(15)$$

$$H_{i,j}^{t+\Delta t} = H_{i,j}^{t} + \rho_l Cp_l \left(T_F - T_{i,j}\right) \quad ...(16)$$

Energy Performances

Thermal Effectiveness of Heat Storage in PCMs

$$\varepsilon_{th} = \frac{Q_{st}}{\int_{t0}^{tc} \varphi_s A_c \, dt} \quad ...(17)$$

With t_0 and t_c hour of the rising and laying down sun

Thermal effectiveness of heat destocking in PCMs

$$\varepsilon_{ext} = \frac{Q_{ext}}{Q_{st}} \quad ...(18)$$

With

$$Q_{ext} = \left(\overline{f_c} - \overline{f_d}\right) m L_{fus} \quad ...(18a)$$

$$Q_{st} = \overline{f_c} \, m L_{fus} \quad ...(18b)$$

where

A_c wall surface subjected to solar flux (m2);

f_c liquid average fraction at the end of the load;

f_d liquid average fraction at the end of the discharge;

L_{fuc} latent heat of fusion for PCMs ($J.Kg^{-1}$) ; 12

m PCM mass (Kg) ;

Q_{ext} quantity of heat extracted PCMs for the period of discharge (J) ;

Q_{est} quantity of latent heat stored in PCM for the period of load (J) ;

t_0 *et* t_c beginning and end of the period of load (s) ;

φ_s solar flux density ($W.m^{-2}$)

Boundary Conditions

Boundary conditions are defined along both axis X and Y.

Following the Y axis, we have:

$$\alpha \left(T_{air} - T_{pcm}\right) = \lambda \left(\frac{\partial T}{\partial X}\right)_{pcm} \quad ...(19)$$

The development of this equation gives us:

$$\alpha\left(T_{air}-T_{IN}\right)=\lambda\left(\frac{T_{IN}-T_{IN-1}}{\Delta X}\right) \quad ...(20)$$

$$\alpha\left(T_{air}-T_{J,1}\right)=\lambda\left(\frac{T_{J,1}-T_{J,2}}{\Delta X}\right) \quad ...(21)$$

Following the X axis, we have:

$$\alpha\left(T_{air}-T_{pcm}\right)=\lambda\left(\frac{\partial T}{\partial Y}\right)_{pcm} \quad ...(22)$$

By analogy with equations 20 and 21, we find:

$$\alpha\left(T_{air}-T_{JN}\right)=\lambda\left(\frac{T_{JN}-T_{JN-1}}{\Delta Y}\right) \quad ...(23)$$

$$\alpha\left(T_{air}-T_{I,1}\right)=\lambda\left(\frac{T_{I,1}-T_{I,2}}{\Delta Y}\right) \quad ...(24)$$

After the discretization of these equations, we find the following dimensionless equations:

Following Y, we have:

$$T_{pcm(1,JJ)}=\frac{\left[\frac{\alpha L}{\lambda_{ref}}\frac{T_{air}}{T_{ref}}+\frac{\lambda_s L}{\lambda_{ref}\Delta X}\frac{T_{pcm(2,JJ)}}{T_{ref}}\right]}{\left[\frac{\alpha L}{\lambda_{ref}}+\frac{\lambda_s L}{\lambda_{ref}\Delta X}\right]} \quad ...(25)$$

$$T_{pcm(IN,JJ)}=\frac{\left[\frac{\alpha L}{\lambda_{ref}}\frac{T_{air}}{T_{ref}}+\frac{\lambda_s L}{\lambda_{ref}\Delta X}\frac{T_{pcm(IN-1,JJ)}}{T_{ref}}\right]}{\left[\frac{\alpha L}{\lambda_{ref}}+\frac{\lambda_s L}{\lambda_{ref}\Delta X}\right]} \quad ...(26)$$

Following X, we have:

$$T_{pcm(II,JJ)}=\frac{\left[\frac{\alpha L}{\lambda_{ref}}\frac{T_{air}}{T_{ref}}+\frac{\lambda_s L}{\lambda_{ref}\Delta Y}\frac{T_{pcm(II,JN-1)}}{T_{ref}}\right]}{\left[\frac{\alpha L}{\lambda_{ref}}+\frac{\lambda_s L}{\lambda_{ref}\Delta Y}\right]} \quad ...(27)$$

$$T_{pcm(II,1)}=\frac{\left[\frac{\alpha L}{\lambda_{ref}}\frac{T_{air}}{T_{ref}}+\frac{\lambda_s L}{\lambda_{ref}\Delta Y}\frac{T_{pcm(II,2)}}{T_{ref}}\right]}{\left[\frac{\alpha L}{\lambda_{ref}}+\frac{\lambda_s L}{\lambda_{ref}\Delta Y}\right]} \quad ...(28)$$

METHODS

For the resolution of the equations in the building and in the phase change material, we used the Gauss and Thomas algorithms respectively.

The systems of algebraic equations obtained by establishing energy balances on the different components of the habitat model are of the form (Kemajou and Mba, 2012):

$$C\frac{dT(t)}{dt}=-K.T(t)+B.\Phi(t) \quad ...(29)$$

with:

T(t) Vector of temperatures at different time-dependent nodes () *Tt t*

C Vector column consisting of thermal capacities at different nodes *C*

K Square matrix composed of thermal conductance *K*

B Matrix coefficient for the different nodes

Φ(*t*) Vector column representing the inputs of the system (thermal excitations)

The equations (5 to 7) are discretized by an implicit finite difference method, whose resolution requires iterative computation. The system is solved by the Gauss algorithm coupled to an iterative method because the transfer coefficients depend on the temperatures of the different building components.

The enthalpy method is applied for the resolution of the heat equation, it is known by its robustness and results from the fact that it makes it possible to determine the temperature field without having recourse to the knowledge of the progression of the front of solidification in the time. It thus makes it possible to solve phase change problems for complex geometries but also when there is a pasty zone. The principle of this method is that for both phases, a single variable, enthalpy H, is used as an unknown and thus reduces the equation system to a single heat transport equation (9 to 16). For this method, generally, the reference temperature is equal to the phase change temperature (melting temperature).

RESULTS AND DISCUSSION

Model Validation

Many validation methods of the model exist, for our case, we validated our model with the experimental study carried out by (Zivkovic and Fujii, 2001) who have made an experimental study of the heat transfers in a parallelepipedic tank filled with PCM (Hydrated salt) soaked in a tank water at a temperature of 60 °C. The walls of this tank are made of stainless steel (100x100x20 mm) and thermally insulated (adiabatic process). The temperature in the middle of the PCM is measured using a K-type thermocouple placed in the center of the tank. The curve in Figure 6 below allows us to say that there is indeed a close qualitative and quantitative relationship between our numerical simulation and the chosen experimental model. The fusion time of our numerical model is long compared to the experimental model, this is due to the fact that the phenomenon of convective heat transfer at the level of the PCM is neglected in the numerical model.

Figure 6: Model Validation

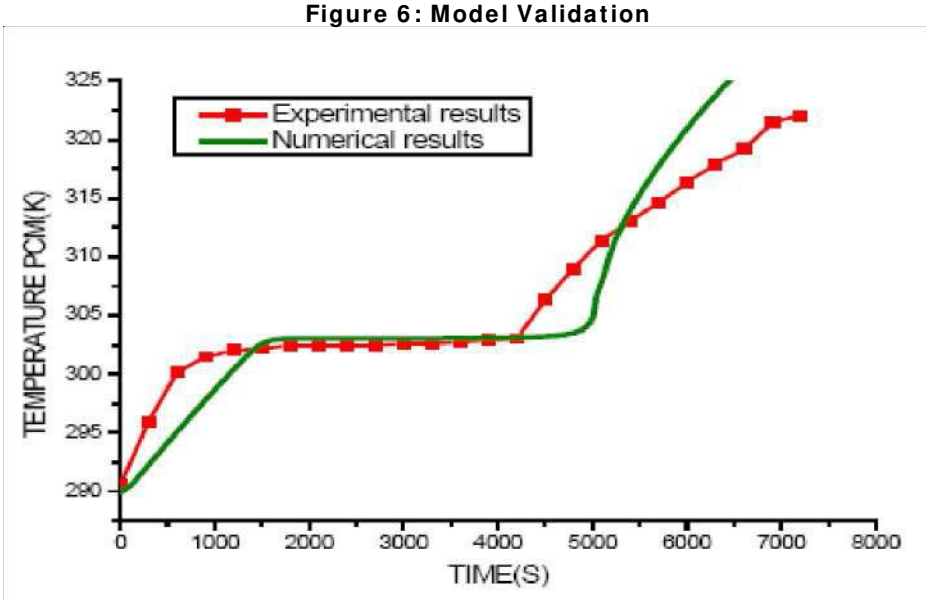

PCM STUDIED

The following results concerning the phase-change material alone have been obtained with the same boundary conditions as the used for validation.

Figure 7 shows the evolution of the phase change for the hydrated salt and paraffin. According to this figure, we find that the hydrated salt has a melting point higher than that of paraffin RT27 with a longer melting time than for paraffin. This indicates that the heat stored in the hydrated salt is important compared to that stored in paraffin RT27. The melting temperatures of these two materials (hydrated salt and Paraffin RT27) are respectively 29.9 °C and 27 °C.

Figure 8 represents the evolution of the heat stored in the phase-change material at the various points chosen for our study over time. On this figure, we find that the extreme points retain much more heat compared to the intermediate points. This is because the height of 16 mm receives the heat first, before returning it to the height of 2 mm which is the last point near the interior of the habitat.

Figure 7: Comparison Between Two-phase Change Materials

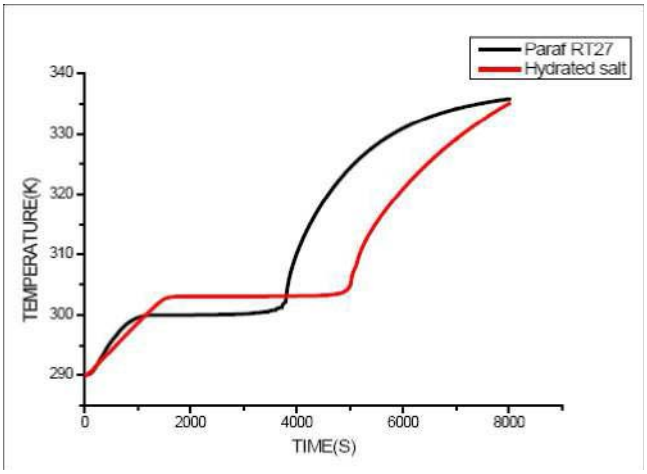

Figure 8: Evolution of the Heat Stored in the PCM at Different Points Over Time

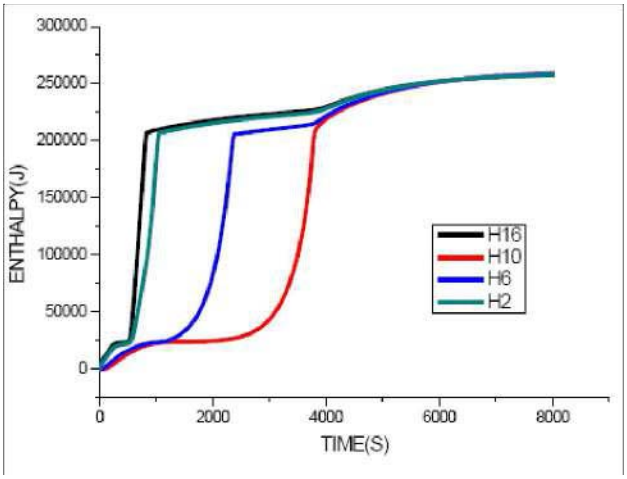

Figure 9 shows the evolution of the heat stored at middle point of the phase change material as a function of the thickness after 8000 second. This figure shows that the stored heat increases according to the variation of the thickness from 5mm up to 20 mm, at 25 mm where the heat is constant and starts to decrease from 30 mm up to 50 mm where the stored heat is less important. So there is less heat stored in the center with an increase in thickness because the heat takes more time longer to reach the center.

HABITAT STUDY

Temperature Distribution

Figure 10 represents the evolution of the air temperature in the enclosure of the habitat with and without phase-change material. According to this figure, we find that the air temperature in modern habitat (with PCM) decreases compared to conventional habitat (without PCM) because the PCM stores the heat during the day and restitutes it during the night, while in the classic habitat, this heat penetrates inside the habitat and the air is overheated. The temperatures observed at 16 h are respectively for a classical habitat and a modern habitat 29.64 °C and 28.71 °C. The ambient air temperature is low compared to the indoor temperatures in the 6 h – 13 h and 23 h – 5 h intervals due to the effect of the sky. The ambient air overheats and exceeds the indoor temperature of the room from 14 h to 22 h for the modern habitat.

Figure 11 illustrates the temperature profiles of the exterior and interior faces of the south wall for habitat with and without PCM. Temperatures observed at the exterior face of the southern wall of conventional habitat dominate those of modern habitat with a difference of 6 °C between maximum temperatures. Temperatures of interior face of southern wall for modern habitat are lower

Figure 9: Heat Stored in the PCM According to the Variation of the Thickness

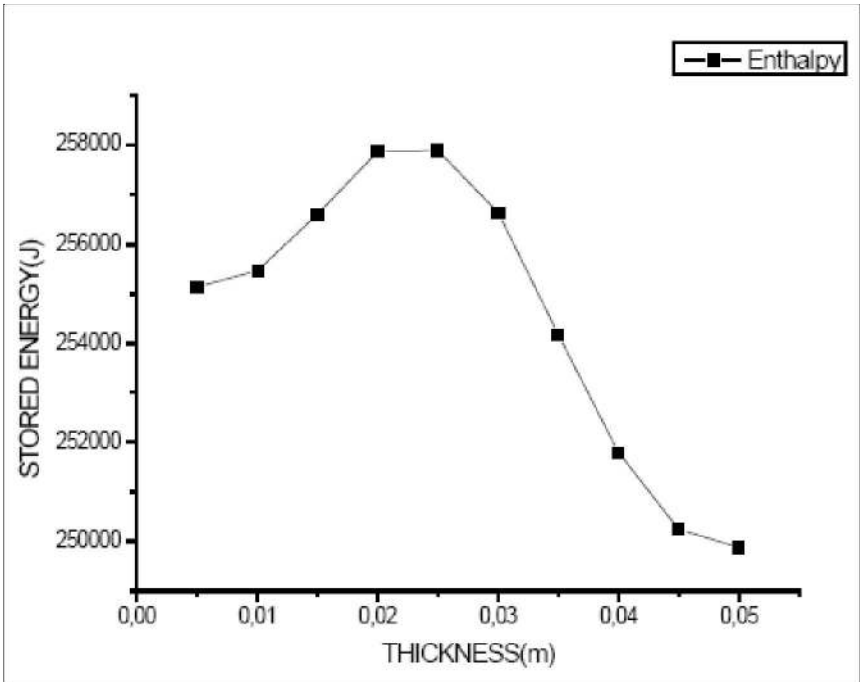

Figure 10: Air Temperature Profile in the Habitat with and Without PCM

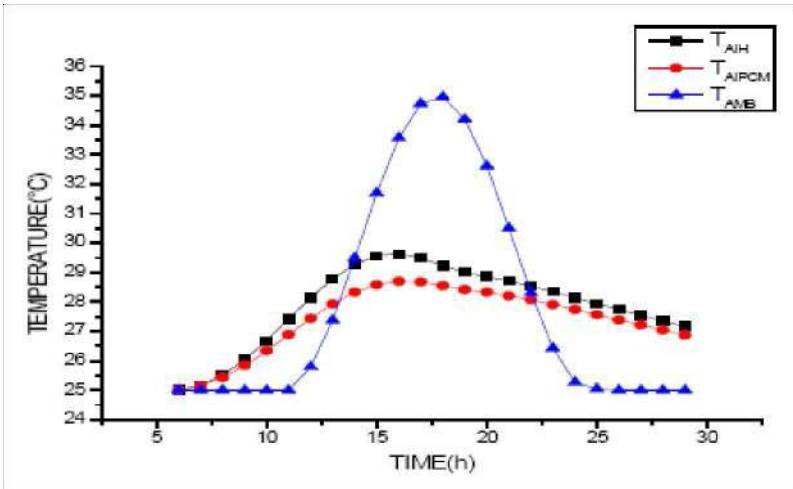

Figure 11: Interior and Exterior Faces Temperatures of Southern Wall with and Without PCM

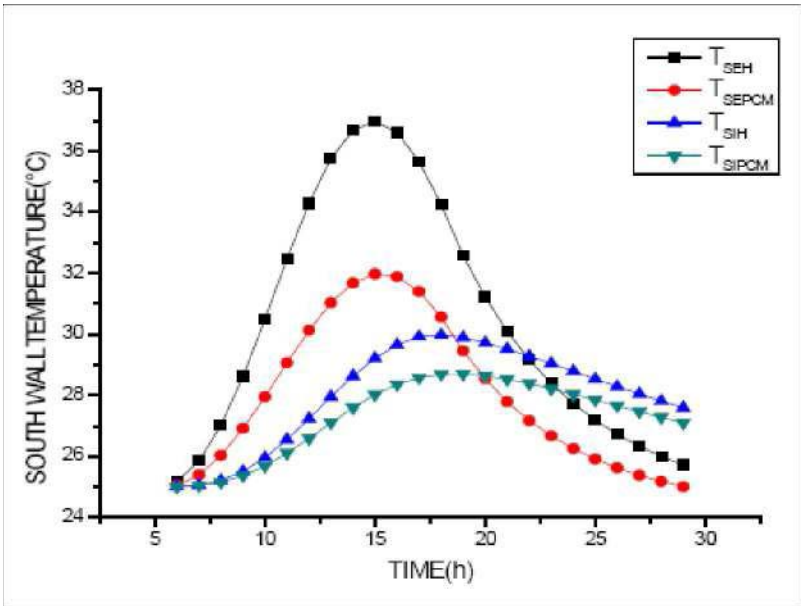

than those of conventional habitat with a difference of about 2 °C. This demonstrates that integrating PCM into habitat provides significant thermal inertia compared to habitat without PCM. The temporal shift between the outdoor and indoor temperatures of the south wall for habitats with and without PCM are respectively 5 h and 4 h.

Figure 12 shows the wall thickness influence on air temperature inside the habitat enclosure with and without PCM. We find that the more the thickness of the wall varies, the greater the thermal inertia and air temperature inside the habitat. By comparing the temperature distributions of the two habitats, we observe that the air temperature decreases in the habitat integrating PCM. This shows that some of the energy provided by the solar flux is stored in the PCM and does not reach the habitat enclosure.

Figure 12: Thickness Wall Influence on Habitat Air Temperature with and Without PCM

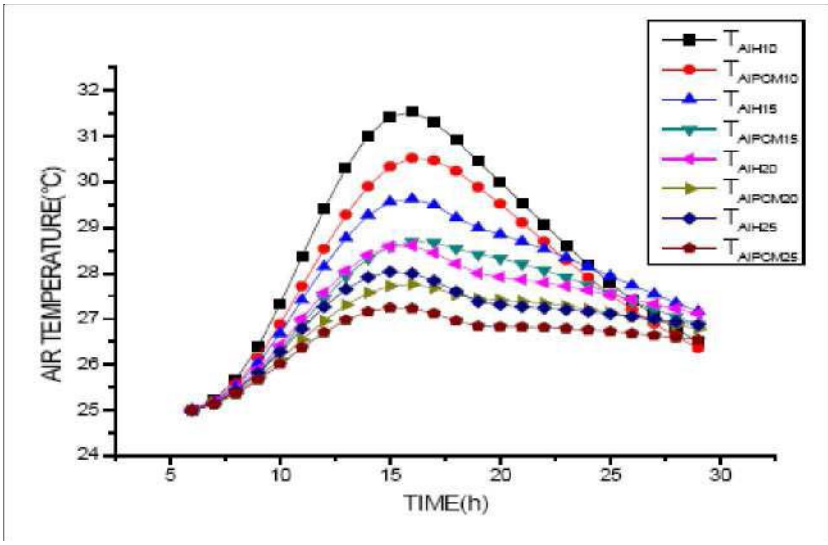

We present in Figure 13 the influence of solar flux on the indoor air temperature with and without PCM for a thickness of the wall fixed at 15 cm. We find that for an important flux, the habitat integrating PCM stores a lot of heat during the day and restitutes it during the night into the enclosure. While the habitat without PCM overheats and the inside temperature rises. We can say that the PCM acts as a temperature damper. For a maximum global heat flux of 1300 $W.m^{-2}$, the maximum air temperature in the habitat without PCM is about 30°C and that of the habitat with PCM is 28°C.

Figure 13: Flux Influence on Indoor Air Temperature with and Without PCM

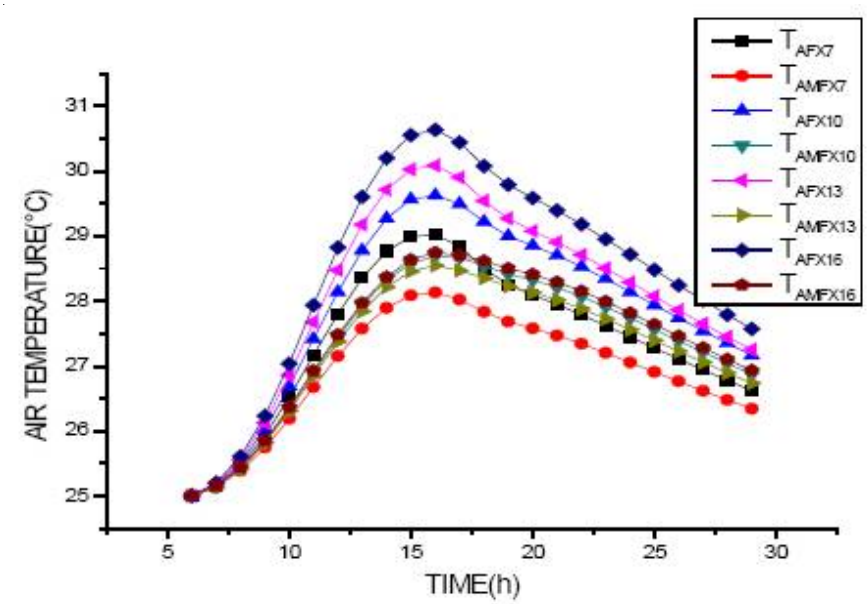

Figure 14 shows the influence of the solar flux on the temperature of the air inside the roof for an habitat with and without PCM with a wall thickness fixed at 15 cm. We note that for an important solar flux the roof of the habitat without phase change material overheats and this causes the rise of the temperature, on the other hand, the roof of the habitat integrating PCM stores a lot of heat during the day to avoid temperature rise. For a maximum heat flux of 1600 W.m-2, the maximum air temperature in the roof of the habitat without PCM is approximately 68 °C and that of the habitat with PCM is 27 °C at 12 h.

We present in Figure 15 the influence of the solar flux on the distribution of the south interior wall temperature of the habitat with and without PCM for a wall thickness fixed at 15 cm. This wall temperature have the same evolution that the solar heat flux. It increases from 6 h, passes through its maximum towards 13 h and then decreases until 18 h. We notice that the wall temperature is less important for the wall of the habitat with phase-change material it means that the latter stores the heat and so the thermal inertia is more important. For a maximum flux of 1600 W.m-2, the maximum temperature of the inner face of the south wall of habitat without PCM is approximately 30 °C and that of habitat with PCM is 28 °C.

Figure 14: Flux Influence on Indoor Roof Air Temperature of Habitat with and Without PCM

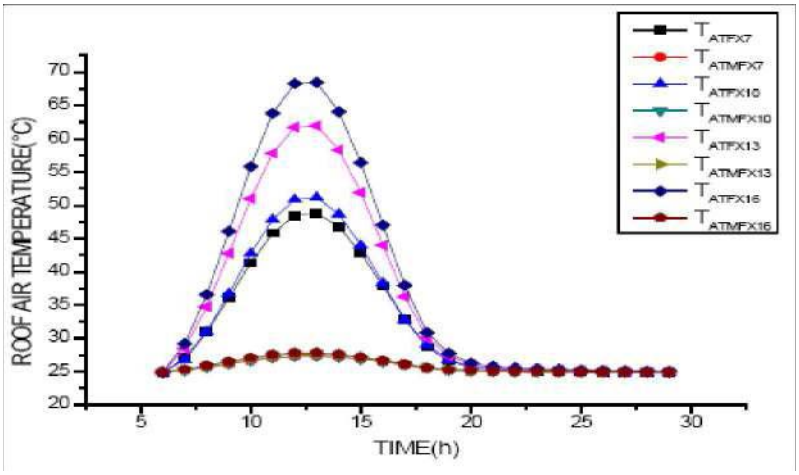

Figure 15: Solar Flux Influence on the South Interior Wall Temperature of Habitat with and Without PCM

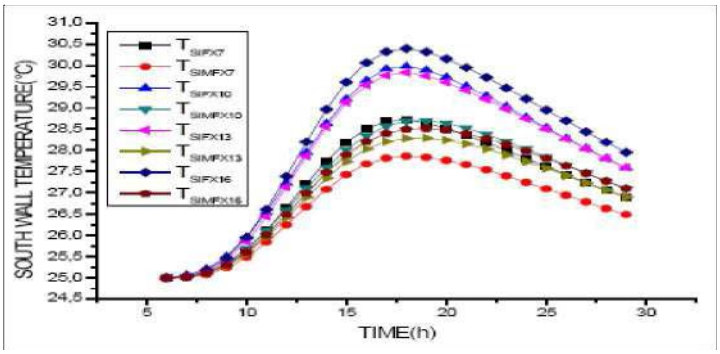

Figure 16 shows the influence of air change rate on air temperature in the enclosure of a habitat with and without PCM. On this figure, we can see that an increase of the air change rate induces an increase of the air temperature. This increase is also present during the night period but is less pronounced for the habitat with phase-change material. This is due to the exchange of warm air from the outside to the interior of the habitat during the day. It is there for necessary to limit the rate of air exchange in the habitat if we want to increase the efficiency of the energy storage in the phase-change material.

Figure 17 shows the influence of solar flux variation on heat storage and discharge efficiency in the phase change material. We find that the storage efficiency decreases with an increase of the solar flux. This is due to the definition of the storage efficiency who has the total solar flux at the denominator. The discharge efficiency also decreases with increasing solar flux. In 20 fact, with a larger solar flux the temperature of the phase-change material greatly exceeds the melting temperature and therefore it takes longer for the re-solidification.

Figure 16: Air Change Rate Influence on Indoor Air Temperature with and Without PCM

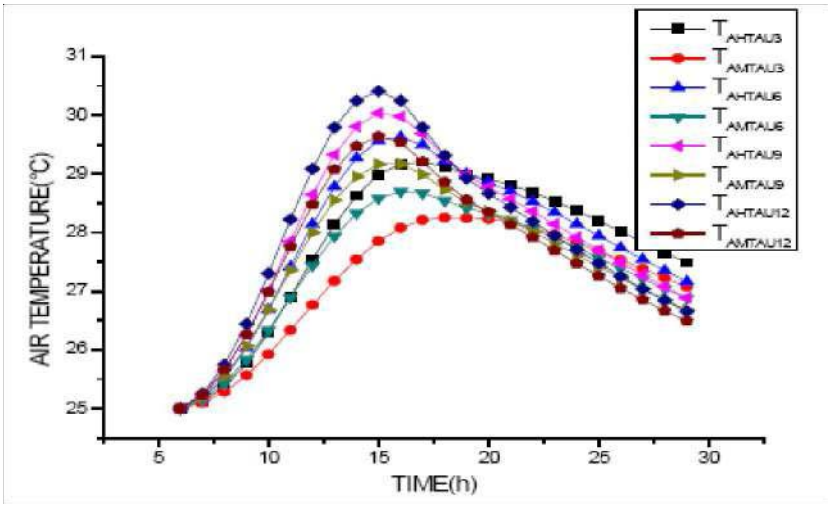

Figure 17: Solar Flux Influence on the Storage and Discharge Efficiency

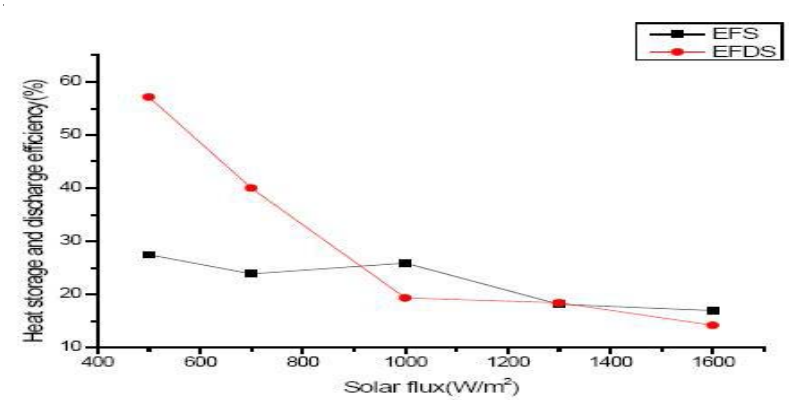

CONCLUSION

We presented a numerical modeling of thermal transfers within a building and heat storage by the enthalpy method in a phase change material. This enabled us to analyze the influence of certain parameters on the thermal behavior of the building. We validated our numerical model with the experimental results proposed by (Zivkovic and Fujii, 2001). For show the utility to use phase-change material, we compared the results obtained for an habitat with and without phase-change material. We have shown the influence of different parameters on the evolution of the temperature inside the enclosure, such as the nature of the phase-change material, the wall thickness and the solar heat flux. The efficiency of storage and discharge of heat and the influence of the variation of certain physical parameters on the distribution of the temperature.

REFERENCES

1. Aadmi M et al., (2013), "*Modélisation du stockage et déstockage d'énergie dans un composite chargé avec un matériau à changement de phase*", *Conference Paper*.
2. Ahmad M (2004), *"Nouveaux Composants actifs pour la gestion Energétique de l'enveloppe légère des bâtiments, Couplage matériaux a changement de phase, super isolation, apports Solaires", Thèse de Doctorat à l'Université Joseph Fourier en Mécanique et Energétique.*
3. Baetens R and *et al.*, (2010), "Phase Change Materials for Building Applications: A state-of-theart Review"*, Energy and Buildings*, Vol. 42, pp. 1361-1368.
4. Bedecarrats J P (2010), "Utilisation Rationnelle De L'énergie Par Les Techniques De Stockage Et De Transport Du Froid Par Chaleur Latente", *Habilitation à diriger les recherches, Université de Pau et des Pays de l'Adour*.
5. Berger X (1984), "Ambiances Radiatives et Confort Thermique", *Comportement Thermique Des Bâtiments*, Vol. 21.
6. Boukli Hacene M E A (2013), "Aspects Energétiques, Economiques et Environnementaux d'une Habitation Ecologique", Thèse de Doctorat en Physique, Université Abou Bekr Belkaid-Tlemcen.
7. Boukli Hacene M A and al., (2011), "Thermal Requirements and Temperatures Evolution in an Ecological House", *Energy Procedia*, pp. 110-121.
8. Brun A (2011), "Amélioration du confort d'été dans les bâtiments à ossature par ventilation de l'enveloppe et stockage thermique", Grenoble.
9. Candas V (2008), "Confort Thermique"*,* Technique de l'ingénieur, traité Génie Energétique, No. BE 9085.
10. Chi-ming L and Shuichi H (2014), "Thermal Performance of an Aluminum Honeycomb Wallboard Incorporating Microencapsulated PCM", *Energy and Buildings*, Vol. 73, pp. 37-47.
11. Fang X and *et al.*, (2008), "Study on Preparation of Montmorillonite-based Composite Phase Change Materials and Their Applications in Thermal Storage Building Materials", *Energy Conversion and Management*, pp. 718-723.
12. Gracia A and Cabeza L F (2015), "Phase Change Materials and Thermal Energy

Storage for Buildings", *Energy and Buildings*, pp. 414-419.

13. Hoy-Yen C and *et al*., (2010), "Review of Passive Solar Heating and Cooling Technologies", *Renewable and Sustainable Energy Reviews*, Vol. 14, pp. 781-789.
14. Hussein J and *et al*., (2014), "Review of Development Survey Of Phase Change Material Models In Building Applications", *Hindawi Publishing Corporation the Scientific World Journal*, p. 11.
15. Kemajou A and Mba L (2012), "Real Impact of The Thermal Inertia on the Internal Ambient Temperature of the Building in the Hot Humid Climate : Simulation and Experimental Study in The City of Douala in Cameroun", *IJRRAS*, Vol 11, pp. 358-367.
16. Khudhair A M and Farid M (2004), "A Review on Energy Conservation in Building Applications With Thermal Storage By Latent Heat Using Phase Change Materials", *Energy Conservation and Management*, Vol. 45, pp. 263-275.
17. Kuznik F and *et al*., (2008), "Optimization of Phase Change Material Wallboard for Building Use", *Applied Thermal Engineering*, Vol. 28, pp. 1291-1298.
18. Manzano-Agugliaro F and *et al*., (2015), "Review of Bioclimatic Architecture Strategies for Achieving Thermal Comfort", *Renewable and Sustainable Energy Reviews*, Vol. 49, pp. 736-755.
19. Neeper D A (2000), "Thermal Dynamics of Wallboard with Latent Heat Storage", Solar Energy, Vol. 68, Issue 5, pp.393-403.
20. Oro E and al., (2012), "Review on Phase Change Materials (PCMs) for Cold Thermal Energy Storage Applications", Vol. 99, pp. 513-533.
21. Ouédraogo I and *et al*., (2007), "Modeling of a Bioclimatimatic Roof Using Natural Ventilation", Research Gate Publication.
22. Pérez-Lombard L and *et al*., (2008), "A Review on Buildings Energy Consumption Information", *Energy and Buildings*, Vol. 40, pp. 394-398.
23. Ramakrishnan S and *et al*., (2017), "Thermal Energy Storage Enhancement of Lightweight Cement Mortars With The Application of Phase Change Materials", *Science Direct, Procedia Engineering*.
24. Soares N and *et al*., (2013), "Review of Passive Pcm Latent Heat Thermal Energy Storage Systems Towards Buildings' Energy Efficiency", *Energy and Buildings*, Vol. 59, pp. 82-103.
25. Socaciu L and al., (2014), "Review on Phase Change Materials for Building Applications", *Leonardo Electronic Journal of Practices and Technologies*, No. 25, pp. 179-194.
26. Tzikopoulos A F and *et al*., (2005), "Modeling Energy Efficiency of Bioclimatic Buildings", *Energy and Building,* Vol. 37, pp. 529-544.
27. Vasilios A and Alan D S (1993), "Mathematical Modeling of Melting and Freezing Processes", Hemisphere Publishing Corporation.
28. Younsi Z *et al*., (2009), "*Etude expérimentale d'un mur trombe-composite à échelle réduite intégrant des matériaux à changement de phase", IXème Colloque Interuniversitaire Franco-Québécois sur la Thermique des Systèmes, Lille*.

29. Zalba B and *et al*., (2003), "Review on Thermal Energy Storage With Phase Change: Materials, Heat Transfer Analysis and Applications", Applied Thermal Engineering, vol. 23, pp. 251-283.

30. Zivkovic B and Fujii I (2001), "An Analysis of Isothermal Phase Change Of Phase Change Material Within Rectangular and Cylindrical Containers", *Solar Energy,* Vol. 70, No. 1, pp. 51-61.

NOMENCLATURE

$h_{r_{sol}}$	Wall- floor radiation coefficient [W.m^{-2}.K^{-1}]
$h_{r_{vc}}$	Wall-celestial vault radiation coefficient [W.m^{-2}.K^{-1}]
T_{vc}	Celestial vault temperature [K]
h_c	Convection transfer coefficient [W.m^{-2}.K^{-1}]
h_r	Radiation transfer coefficient [W.m^{-2}.K^{-1}]
h_d	Conduction transfer coefficient [W.m^{-2}.K^{-1}]
K	Thermal conductivity [W.m^{-1}.K^{-1}]
h_{cex}	Convection transfer coefficient at a outer wall [W.m^{-2}.K^{-1}]
$h_{ri \rightarrow pi}$	Radiation transfer coefficient between two walls [W.m^{-2}.K^{-1}]
α_{tex}	Absorption coefficient of the outer cover
φ_{tex}	Heat flux density at the outer wall [W.m^{-2}]
T_{amb}	Ambient temperature [K]
T_{air}	Air temperature [K]
T_{flor}	Floor temperature [K]
Ep	Wall thickness [m]
Φ_{ra}	Heat flux exchange by air renewal [J.h^{-1}]
H	Enthalpy [J]
M_{tex}	Mass of the outdoor roof [Kg]
$C_{p_{tex}}$	Thermal capacity of the outdoor roof [J.Kg^{-1}.K^{-1}]
T_{ti}	Temperature of the internal face of the roof [°C]
T_{tex}	Temperature of the external face of the roof [°C]
$h_{r_{vc,pex}}$	Radiation transfer coefficient between the sky and the outer wall [W.m^{-2}.K^{-1}]
$h_{r_{flor,pex}}$	Radiation transfer coefficient between the floor and outer wall [W.m^{-2}.K^{-1}]
$h_{ci,pi}$	Convection transfer coefficient between the air and the inner wall [W.m^{-2}.K^{-1}]
$h_{ri \rightarrow pi}$	Radiation transfer coefficient between two internal walls [W.m^{-2}.K^{-1}]
T_{airh}	Air temperature inside the habitat [°C]
F_i	Form factor between two walls
BTS	Stabilized clay bricks 3

PCM	Phase-change material
RGH	Global radiation [W/m^2]
EFS	Storage efficiency [%]
EFDS	Discharge efficiency [%]
TEMP	Ambient temperature [K]
T_{AIH}	Air temperature inside the habitat without PCM [°C]
T_{AIPCM}	Air temperature inside the habitat with PCM [°C]
T_{AMB}	Ambient temperature [K]
T_{SEH}	Outside south wall temperature of habitat without PCM [°C]
T_{SEPCM}	Outside south wall temperature of habitat with PCM [°C]
T_{SIH}	Interior south wall temperature of habitat without PCM [°C]
T_{SIPCM}	Interior south wall temperature of habitat with PCM [°C]
T_{AIH10}	Air temperature inside the home without PCM for wall thickness set at 10 cm [°C]
$T_{AIPCM15}$	Air temperature inside the home with PCM for wall thickness set at 15 cm [°C]
T_{AFX7}	Air temperature inside the home without PCM for a maximum flux of 700 W / m2 [°C]
T_{AMFX10}	Air temperature inside the home with PCM for a maximum flux of 1000 W/m^2 [°C]
T_{ATFX7}	Air temperature inside the roof of the home without PCM for a maximum flux of 700 W / m^2 [°C]
$T_{ATMFX16}$	Air temperature inside the roof of the home with PCM for a maximum flux of 1600 W / m^2 [°C]
T_{SIFX7}	Interior south wall temperature of the home without PCM for a maximum flux of 700 W / m^2 [°C]
$T_{SIMFX13}$	Interior south wall temperature of the home with PCM for a maximum flux of 1300 W / m^2 [°C]
T_{AHTAU3}	Air temperature inside the home without PCM for an air change rate set at 3 / 24h [°C]
T_{AMTAU9}	Air temperature inside the home with PCM for an air change rate set at 9 / 24h [°C]

H_{16}	Enthalpy at the height of 16 mm [J]
H_2	Enthalpy at the height of 2 mm [J]
L	PCM length[m]
λ_{ref}	Reference thermal conductivity of the PCM [$W.m^{-1}.K^{-1}$]
λ_s	Thermal conductivity of the solid PCM [$W.m^{-1}.K^{-1}$]
T_{ref}	Reference temperature [K]
$T_{pcm(IN,JJ)}$	Temperature at the point IN and JJ [K]
α	Convection coefficient [$W.m^{-2}.K^{-1}$]
ΔX and ΔY	andSpace steps [m]